

UDC 539.194

**STRUCTURE AND STABILITY OF ENDOHEDRAL COMPLEXES $^{4/2}X@(\text{HAlNH})_{12}$
(X = N, P, As, C⁻, Si⁻)**

© 2011 C.-Yu. Zhang*, X. Zhao, J. Zhang, B.-Q. Wang

*Department of Chemistry and Material Science, Shanxi Normal University, Linfen 041004, China**Received February, 28, 2010*

The structures of a closo-hedral cluster (HAlNH)₁₂ and endohedral complexes $^{4/2}X@(\text{HAlNH})_{12}$ (X = N, P, As, C⁻, Si⁻) are studied by density functional theory (DFT) at the B3LYP/6-31G(*d*) level. The geometries, natural bond orbital (NBO), vibrational frequency (ν_1), energetic parameters, magnetic shielding constants (σ), and nucleus independent chemical shifts (NICSs) are discussed. It is found that all guest species are minima at the cage center. Inclusion energies (ΔE_{inc}) of all species are negative except those of ^4N and $^{4/2}\text{P}$. In all species, the endohedral quartet states (^4X) are energetically less favorable than their doublet states (^2X). The calculations predict that caged X states only donate <0.50 e to the cage and preserve their unencapsulated ground states.

Keywords: density functional theory, endohedral complexes, inclusion energy, quartet state, doublet state.

INTRODUCTION

Representing a link between isolated molecules and bulk phase clusters of aluminium and nitrogen, Al_xN_y have drawn increasing attention during last years. This is mainly because solid AlN with its unusual specific physical properties is of great interest to microelectronic, ceramic, material, and surface sciences [1—9]. (AlN)₁₂ is a ground state structure with T_h symmetry [10]. The hydrogenation reaction of (AlN)₁₂ is exothermal with the hydrogenation heat (ΔH_{h}) of -127.813 kJ/mol [11], so its hydride (HAlNH)₁₂ structure should be more stable. In addition, since this type of cage has a relatively larger interspace, the cage break should not occur when guest atoms are introduced. Thus, this type of compounds could be designed as novel polyhedral structures. Herein we calculate the structure and stability of the (HAlNH)₁₂ cluster complex and its endohedral complexes $^{4/2}X@(\text{HAlNH})_{12}$ (X = N, P, As, C⁻, Si⁻), and the results could provide a valuable reference for the synthesis of novel structural materials.

COMPUTATIONAL METHODS

All calculations were carried out using the parallel version of the Gaussian 03 software package [12]. The configurations of the (HAlNH)₁₂ complex and $^{4/2}X@(\text{HAlNH})_{12}$ (X = N, P, As, C⁻, Si⁻) endohedral complexes were optimized by the DFT method at the B3LYP/6-31G(*d*) level. The optimized structures were characterized by frequency calculations as the energy minima (zero imaginary frequencies: $N_{\text{imag}} = 0$). Atomic charges (q) and spin densities (S) were evaluated using the natural bond orbital (NBO) analysis [13]. Thermodynamic parameters (ΔE_{inc} , ΔE_{def}), magnetic shielding constant (σ), and nuclear independent chemical shift (NICS) were computed at the same level. The results are presented in Tables 1—4, and the optimized structures are shown in Fig. 1.

* E-mail: zhaoxiamei1985@163.com

RESULTS AND DISCUSSION

(HAINH)₁₂ and (HAINH)₁₂⁻. As found previously, (HAINH)₁₂ in T_h symmetry (Fig. 1, *a*) is an energy minimum structure ($N_{\text{imag}} = 0$). According to the NBO analysis, both Al and N atoms on the skeleton of the (HAINH)₁₂ complex form a 4-coordinated cage structure with an sp^x ($x = 2 \sim 4$) hybrid. Al is an electron-deficit atom, correspondingly, N has relatively stronger electronegativity, so the (HAINH)₁₂ compound has obvious ability to receive electrons. In the present work, the structure optimization and energy calculation of (HAINH)₁₂, and (HAINH)₁₂⁻ were carried out. As shown in Fig. 2, we can see that the (HAINH)₁₂ cage has non-degenerate LUMO-133 (A_g) and distributes fully around the cage center, therefore the cage is able to host one additional electron into the LUMO without lowe-

Table 1

Bond Lengths (R , Å) of (HAINH)₁₂^{0/-} and X@(HAINH)₁₂ clusters

Cluster	$R(\text{X}-\text{N})$	$R(\text{X}-\text{Al})$	$R(\text{N}-\text{Al})^a$	$R(\text{N}-\text{Al})^b$	$R(\text{N}-\text{H})$	$R(\text{Al}-\text{H})$
(HAINH) ₁₂	(2.970)	(3.100)	1.892	1.949	1.027	1.590
(HAINH) ₁₂ ⁻	(3.010)	(3.060)	1.886	1.949	1.028	1.610
⁴ N@(HAINH) ₁₂	2.979	3.112	1.897	1.953	1.027	1.591
² N@(HAINH) ₁₂	2.979	3.111	1.897	1.952	1.027	1.592
⁴ P@(HAINH) ₁₂	3.005	3.127	1.910	1.964	1.028	1.591
² P@(HAINH) ₁₂	3.005	3.126	1.910	1.964	1.028	1.591
⁴ As@(HAINH) ₁₂	3.005	3.124	1.907	1.965	1.028	1.591
² As@(HAINH) ₁₂	3.005	3.123	1.906	1.965	1.029	1.590
⁴ C ⁻ @(HAINH) ₁₂	3.019	3.062	1.890	1.947	1.025	1.610
² C ⁻ @(HAINH) ₁₂	3.021	3.061	1.889	1.947	1.025	1.610
⁴ Si ⁻ @(HAINH) ₁₂	3.052	3.087	1.908	1.964	1.028	1.609
² Si ⁻ @(HAINH) ₁₂	3.052	3.086	1.908	1.964	1.028	1.608

^a The N—Al bond fusing two 6-membered rings.

^b The N—Al bond between the 4- and 6-membered rings.

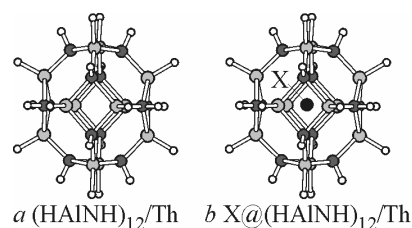
The numbers in parentheses represent the distance from the cage center to a vertex, N or Al.

Table 2

The natural charges (q) and spin densities $S_X(e)$ of (HAINH)₁₂^{0/-} and X@(HAINH)₁₂ clusters

Cluster	q_X	S_X	q_N	q_{Al}	$q_{H(N)}$	$q_{H(Al)}$
(HAINH) ₁₂			-1.730	1.672	0.446	-0.389
(HAINH) ₁₂ ⁻			-1.742	1.643	0.431	-0.415
⁴ N@(HAINH) ₁₂	0.114	2.879	-1.736	1.670	0.446	-0.390
² N@(HAINH) ₁₂	0.101	0.963	-1.736	1.670	0.446	-0.390
⁴ P@(HAINH) ₁₂	0.057	2.746	-1.733	1.672	0.446	-0.391
² P@(HAINH) ₁₂	0.045	0.916	-1.732	1.672	0.447	-0.390
⁴ As@(HAINH) ₁₂	0.127	2.687	-1.738	1.669	0.446	-0.391
² As@(HAINH) ₁₂	0.119	0.897	-1.735	1.669	0.446	-0.391
⁴ C ⁻ @(HAINH) ₁₂	-0.522	2.664	-1.736	1.681	0.434	-0.419
² C ⁻ @(HAINH) ₁₂	-0.494	0.895	-1.735	1.680	0.432	-0.418
⁴ Si ⁻ @(HAINH) ₁₂	-0.501	2.832	-1.732	1.676	0.432	-0.417
² Si ⁻ @(HAINH) ₁₂	-0.494	0.945	-1.732	1.675	0.432	-0.417

Fig. 1. Optimized geometric configurations of (a) $(\text{HAlNH})_{12}$ and (b) $X@(\text{HAlNH})_{12}$ cages



ring the high symmetry. Indeed, the $(\text{HAlNH})_{12}^-$ cage in T_h symmetry is an energy minimum on the B3LYP/6-31G* potential energy surface. As compared to the parent $(\text{HAlNH})_{12}$ cage, the energy reduces slightly, with the values being -3581.9873 and -3581.9898 a.u. respectively. On the other hand, in Tables 1 and 2, the skeleton of the cage swells slightly and tends to be a sphere. Because of the hybrid bonding effect of N and Al, the 4- and 6-membered rings both deviate from the plane. When an electron was added, the H atoms bound to negative N (-1.730 e) all get electron of 0.015 e correspondingly; those bonded to positive Al (1.672 e) all obtain 0.026 e. Because N and Al obtain different number of electrons, i.e. Al obtains more electrons than N (0.029 vs 0.012 e), therefore, the ionicity of the N—Al bond weakens slightly and at the meantime, their bond distances also change. In detail, N—Al bond distances on the 6/6 ring decrease, and those on the 4/6 ring generally do not have any change, but periphery N—H and Al—H bond distances increase. The partial reason is that the antibonding orbitals of periphery N—H and Al—H bonds accepted electrons (0.002 e/Al—H* and 0.006 e/N—H*), and thus the bonds became weaker and longer. The distance between the cage center and the apex N atom increases; on the contrary, that from the cage center to the apex Al atom decreases. Consequently, the rings on the cage surface tend to be a plane. This indicates that the bond angles (N—Al—N) of the 6-membered rings turn bigger after getting electrons, namely N—Al—N increases from 114.3 to 117.6° . If the electrons are removed from $(\text{HAlNH})_{12}$, according to the Jahn-Teller effect, degeneracy of HOMO (T_g) is eliminated, and the symmetry decreases resulting in the configuration changes. Thus, the $(\text{HAlNH})_{12}$ cage structure with T_h symmetry could provide electrons to some extent and could be used as electron acceptor; the adiabatic electron affinity (EA) was calculated for attaching one electron to form $(\text{HAlNH})_{12}^-$ (EA = 6.56 kJ/mol) [14]. Therefore, the addition of one electron does not necessarily lead to symmetry lowering, and such a novel structural model of $(\text{HAlNH})_{12}$ can significantly stabilize the capsulated guests.

$^{4/2}X@(\text{HAlNH})_{12}$ ($X = \text{N, P, As, C}^-, \text{Si}^-$). **Geometric Configuration and Charge Distribution.** When a $^{4/2}X$ guest is introduced into the cage (Fig. 1, b), part of electrons will transfer to the cage skeleton. For the atomic series (N, P, As) the number of transferred electrons of quartet states (4X) is slightly more than that of doublet states (2X) (Table 2), whereas it is reverse for C^- and Si^- negative species. There is negligible electron transfer between the guests and the cage framework (Table 2); the spin densities (S_X) of $^{4/2}X$ ($X = \text{N, P, As, C}^-, \text{Si}^-$) generally do not have larger changes, with spin densities of $2.664 \sim 2.879$ e for quartet states (4X) and $0.895 \sim 0.963$ e for doublet states (2X), thus it still can be considered to approximately pre-

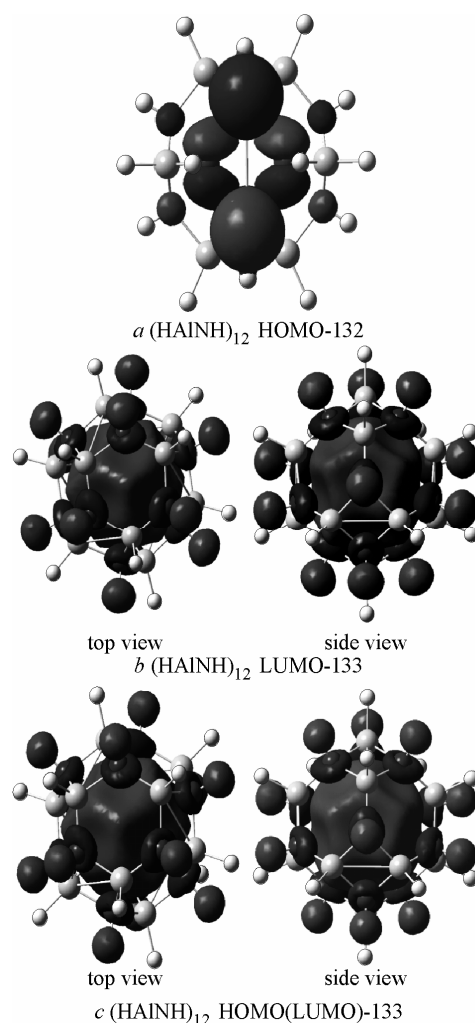


Fig. 2. HOMO and LUMO plots of $(\text{HAlNH})_{12}$ (a, b) and $(\text{HAlNH})_{12}^-$ (c)

Table 3

Total energies E_T (a.u.), lowest vibrational frequencies ν_1 (cm^{-1}), zero-point energy (eV), gap ΔE_g (eV), inclusion energies ΔE_{inc} (kJ/mol) and deformation energies ΔE_{def} (kJ/mol)

Cluster	E_T	ν_1	ZPE	ΔE_g	ΔE_{inc}^a	ΔE_{def}^b
(HAINH) ₁₂	-3581.9873	140.5	8.11	7.12		0.0000
(HAINH) ₁₂ ⁻	-3581.9898	133.2	8.01	2.07(β)	-6.5637	60.1239
⁴ N@(HAINH) ₁₂	-3636.5619	147.4	8.13	7.54	25.9924	-6.8263
² N@(HAINH) ₁₂	-3636.5237	145.1	8.11	2.09	-150.7037	-6.8263
⁴ P@(HAINH) ₁₂	-3923.1802	152.7	8.10	7.44	171.1826	1.5753
² P@(HAINH) ₁₂	-3923.1599	152.4	8.09	2.70	56.4482	1.5753
⁴ As@(HAINH) ₁₂	-5815.6705	149.0	8.11	6.98	-11.0271	1.8378
² As@(HAINH) ₁₂	-5815.6508	140.0	8.08	2.39	-21.0040	2.1004
⁴ C ⁻ @(HAINH) ₁₂	-3619.9789	136.3	8.16	6.15	-386.7361	58.0235
² C ⁻ @(HAINH) ₁₂	-3619.9551	124.8	8.15	3.41	-521.9493	61.9618
⁴ Si ⁻ @(HAINH) ₁₂	-3871.4036	149.4	8.07	4.90	-25.7300	75.6144
² Si ⁻ @(HAINH) ₁₂	-3871.3888	124.7	8.04	2.22	-107.1204	76.9271

^a Inclusion energy: $\Delta E_{\text{inc}} = E[\text{X}@\text{(HAINH)}_{12}] - E(\text{X}) - E[\text{(HAINH)}_{12}]$.

^b $\Delta E_{\text{def}} = E(\text{HAINH})_{12}(\text{strain}) - E(\text{HAINH})_{12}$ is the deformation energies of cage (HAINH)₁₂ due to X or e insertion.

Table 4

Magnetic shielding constants (σ) and Nucleus independent chemical shifts (NICS) of clusters

Cluster	NICS ^a		σ		
	4-ring	6-ring	X	Al	N
(HAINH) ₁₂	-4.40	-0.40	(-0.64)	487.38	204.58
(HAINH) ₁₂ ⁻	-4.49	0.03	(3.25)	493.62	202.72
⁴ N@(HAINH) ₁₂	-4.32	-0.21	271.17	486.60	203.71
² N@(HAINH) ₁₂	-4.89	1.85	-1963.24	486.89	205.31
⁴ P@(HAINH) ₁₂	-4.27	0.16	751.42	487.01	197.84
² P@(HAINH) ₁₂	-4.20	2.99	-3683.03	486.99	207.60
⁴ As@(HAINH) ₁₂	-4.30	0.17	2503.74	487.81	197.48
² As@(HAINH) ₁₂	-4.15	-5.84	-8238.16	487.65	208.10
⁴ C ⁻ @(HAINH) ₁₂	-4.26	-0.05	193.29	494.62	202.91
² C ⁻ @(HAINH) ₁₂	-2.80	-0.18	-1045.76	493.67	209.65
⁴ Si ⁻ @(HAINH) ₁₂	-4.20	0.18	674.72	496.60	195.96
² Si ⁻ @(HAINH) ₁₂	-4.90	-0.13	-2097.75	493.91	209.10

^a The NICS values were calculated at the center a face (0) of 4-ring and 6-ring respectively. The numbers in parentheses represent the σ values of cage center.

serve its atomic ground state. So, the conclusion can be drawn that the interaction between the guest atom X and the (HAINH)₁₂ complex is weak, and various bond lengths of the cage skeleton do not largely change (Table 1).

Energy Parameters and Stability. The harmonic frequency of $^{4/2}X@(\text{HAINH})_{12}$ ($X = \text{N, P, As, C}^-, \text{Si}^-$) cage structure was calculated by the B3LYP/6-31G* method. The lowest vibrational frequency ν_1 could reflect whether the imaginary frequency exists in the structure or not. As the calculation results show, all ν_1 are positive ($N_{\text{img}} = 0$) suggesting that the configuration of the complex with T_h symmetry locates at the stable position of the potential energy surface (PES) and represents a stable structure. Since the skeleton vibrational frequency is sensitive to a change in the molecular structure, this series of compounds could be identified by the characteristic spectrum and provide a theoretical reference for experimental synthesis.

As expected, the total energies of the doublet state of $^2X@(\text{HAINH})_{12}$ ($X = \text{N, P, As, C}^-, \text{Si}^-$) was more than those of the quartet state of $^4X@(\text{HAINH})_{12}$ ($X = \text{N, P, As, C}^-, \text{Si}^-$); the increased values are about 0.01 ~ 0.04 a.u. A comparable trend is observed for the HOMO-LUMO energy gap (ΔE_g); ΔE_g of double states decreases by 3.84 eV in the average value.

Inclusion energy ΔE_{inc} . ΔE_{inc} denotes the energy change in the reaction $X + (\text{HAINH})_{12} \rightarrow X@(\text{HAINH})_{12}$. As shown in Table 3, all ΔE_{inc} are negative except those of ^4N and $^{4/2}\text{P}$, thus indicating that the embedding of the X atom into the cage is an exothermal process and does not need energy to promote it. In addition, due to a larger interspace of the cage, an efficient bond between the X atom at the central position and atoms at the cage face could not exist, and the interaction among them represents an obvious nonbonding property. This long-range interaction consists mainly of electrostatic and repulsive interactions caused by electron cloud overlapping. In Table 2, charges transferred on X guests are relatively small ($<0.5 e$), so the electrostatic interaction is relatively weaker, and the repulsive interaction caused by electron cloud overlapping is dominating.

From the viewpoint of thermodynamics, ΔE_{inc} of the double states are more negative than those of the quartet states (Table 3). This is due to that the energy of the double free state 2X is higher relative to that of the quartet free state 4X ; once caged ΔE_{inc} of $^2X@(\text{HAINH})_{12}$ complexes becomes more exothermic, so a comprehensive conclusion could be drawn that the inclusion energy ΔE_{inc} of the double state is relatively more negative. For example, ΔE_{inc} of $^4\text{N}@(\text{HAINH})_{12}$ is positive (26.0 kJ/mol), whereas that of $^2\text{N}@(\text{HAINH})_{12}$ is negative (-150.7 kJ/mol); ΔE_{inc} of $^2\text{P}@(\text{HAINH})_{12}$ is less positive than that of $^4\text{P}@(\text{HAINH})_{12}$ (56.4 vs. 171.2 kJ/mol), and ΔE_{inc} of $^2\text{As}@(\text{HAINH})_{12}$ is more negative than that of $^4\text{As}@(\text{HAINH})_{12}$ (-21.0 vs. -11.0 kJ/mol) respectively. Furthermore, negative ΔE_{inc} in Table 3 reveal that the process of C^- and Si^- insertion is exothermic (-386.7/ $^4\text{C}^-$ vs. -521.9 kJ/mol/ $^2\text{C}^-$ and -25.7/ $^4\text{Si}^-$ vs. -107.1 kJ/mol/ $^2\text{Si}^-$) indicating that the corresponding encapsulation is energetically favorable.

Deformation energy ΔE_{def} . ΔE_{def} is the energy change in the parent cage due to X or e insertion. We can see from Table 3 that when an electron is included in the cage, the rings on the cage surface tend to be planar; which results in further enhancement of the bond tension and an increase in the ΔE_{def} value (60.1 kJ/mol).

For the same reason discussed above, encapsulated $^{4/2}\text{C}^-$ and $^{4/2}\text{Si}^-$ anions donated more electrons ($\sim 0.5 e$) to the cage skeletal anti-bonding (Al—H* and N—H*) orbitals, which leads to an increase in their cage deformation energy (ΔE_{def}), namely the ΔE_{def} value of atomic series (N, P, and As) is -6.8 ~ 2.1 kJ/mol, while for the anions series (C^- and Si^-), ΔE_{def} is 58.0 ~ 77.0 kJ/mol. As compared to the inclusion energy ΔE_{inc} , this type of the energy change caused by the allosteric effect is not very large. During the embedding of X and its transferring in or out of the cage, the deformation energy ΔE_{def} is only a small part of the releasing energy, and it is not a dominating factor affecting the thermodynamic and dynamic stability.

NICS and the Magnetic Shielding Constant (σ). The NMR data based on B3LYP/6-31G(d) of the complexes are listed in Table 4. The analysis was carried out as follows.

Nuclear independent chemical shift (NICS) values could be used as the aromatic criterion [15]. A negative value of NICS indicates that it has aromaticity, and a positive one suggests anti-aromaticity. The NICS value of the central position in the $(\text{HAINH})_{12}$ cage is 0.64, which denotes weak anti-aromaticity and no shielding effect on the central position. Similarly, 6-membered rings of the cage surface are also non-aromatic (NICS = -0.05 ~ 2.99, except that of ^2As). However, aromati-

city is exhibited in the centres of 4-membered rings of the cage surface. The 4-membered ring is relatively smaller with a stronger overlap of electron cloud due to the formed Al—Al bond, so the centre position has stronger aromaticity and the magnetic shielding effect. When an X atom is introduced into the cage, the aromaticity change is generally the same as that of the (HAlNH)₁₂ cage surface, which further proves that the interaction between the guest atom X and the (HAlNH)₁₂ cluster occurs mainly in the cage.

Magnetic shielding constant (σ) values at the centre of the parent and (HAlNH)₁₂⁻ cage are -0.64 and 3.25 ppm [16]; the relative chemical shift $\delta = -3.89$ ppm [$\delta = \sigma(\text{freeX}) - \sigma(\text{endoX})$], and the magnetic shielding effect is enhanced. The σ values of a free X atom are as follows: ⁴N: 324.73 ppm, ⁴P: 960.52 ppm, ⁴As: 2869.84 ppm, ⁴C⁻: 268.83 ppm, ⁴Si⁻: 878.79; ²N: -2642.18 ppm, ²P: -21413.80 ppm, ²As: -10195.60 ppm, ²C⁻: -1902.53 ppm, ²Si⁻: -2580.21 ppm. When quartet ground-state atoms are embedded in the cage, their σ values decrease (Table 4). Their relative chemical shifts (δ) are: $\delta^4\text{N}$: 53.56 ppm (16 %), $\delta^4\text{P}$: 209.10 ppm (22 %), $\delta^4\text{As}$: 366.10 ppm (13 %), $\delta^4\text{C}^-$: 75.54 ppm (28 %), $\delta^4\text{Si}^-$: 204.07 ppm (23 %). The positive sign of the chemical shifts (δ) is due to the deshielding effect of the cage. The above values are all positive, thus suggesting the occurrence of charge transfer and weakening of the magnetic shielding effect. When doublet state atoms are embedded in the cage, the σ values increase (Table 4), and their relative chemical shifts (δ) are: $\delta^2\text{N}$: -678.93 ppm (26 %), $\delta^2\text{P}$: -17730.77 ppm (83 %), $\delta^2\text{As}$: -1957.44 ppm (19 %), $\delta^2\text{C}^-$: -856.77 ppm (45 %), $\delta^2\text{Si}^-$: -482.46 ppm (19 %). These values are all negative, thus suggesting the enhanced magnetic shielding effect when the doublet state atoms are inserted in the cage. This change order is consistent with the inclusion energy ΔE_{inc} of the X guest, namely ΔE_{inc} of the double state is comparably more negative.

On the other hand, in Table 4, the σ values of Al and N atoms in the (HAlNH)₁₂ complex are 487.38 and 204.58 ppm respectively. After introducing the guest atom X, both Al and N atoms obtain a small number of electrons, so the σ values of Al and N atoms slightly change.

CONCLUSIONS

The (HAlNH)₁₂ cluster with T_h symmetry is a stable structure (N_{img} = 0) and has the ability to store electrons, therefore, the (HAlNH)₁₂⁻ cage in T_h symmetry is an energy minimum on the B3LYP/6-31G* potential energy surface. As compared to the parent cage (HAlNH)₁₂, the energy is slightly reduced. After the insertion of guest species ^{4/2}X, the obtained endohedral complexes ^{4/2}X@(HAlNH)₁₂ (X = N, P, As, C⁻, Si⁻) are still stable and keep T_h symmetry. There is negligible electron (< 0.5 e) transfer between the guests and the cage framework; the spin densities (S_X) of ^{4/2}X (X = N, P, As, C⁻, Si⁻) generally do not have large changes, thus it still can be considered to approximately preserve its atomic ground state, and furthermore, the result predicts that the parent cage has the stored magnetic energy. From the viewpoint of thermodynamics and with regard to changes in several energy parameters, the conclusion could be drawn that the main factor affecting the stability is the cage effect between ^{4/2}X guests and the (HAlNH)₁₂ complex. Furthermore, the inclusion energy (ΔE_{inc}) also depends on this effect. So, a comprehensive conclusion could be drawn that the ⁴X@(HAlNH)₁₂ quartet states complexes have relatively higher energies (ΔE_{inc}) and the double state structure of ²X@(HAlNH)₁₂ complexes is stable with the relatively lower inclusion energy (ΔE_{inc}); this change order is consistent with the relative chemical shifts (δ) of the X guests.

Acknowledgement. This work was supported by the Natural Science Foundation of China (20341005) and by the Natural Science Foundation of Shanxi Province (2007011028) China.

REFERENCES

1. Sun Q., Wang Q., Gong X.G. et al. // Eur. Phys. J.D. – 2002. – **18**. – P. 77.
2. Andrews L., Zhou M., Chertihin G.V. et al. // J. Phys. Chem. A. – 2000. – **104**. – P. 1656.
3. Kandalam A.K., Pandey R., Blanco M.A. et al. // J. Phys. Chem. B. – 2000. – **104**. – P. 4361.
4. Sheppard L.M. // Amer. Ceram. Soc. Bull. – 1990. – **69**. – P. 1801.
5. Ponce F.A., Bour D.P. // Nature. – 1997. – **386**. – P. 351.

6. Jackson T.B., Virkar A.V., More K.L. et al. // J. Amer. Ceram. Soc. – 1997. – **80**. – P. 1421.
7. Moura F.J., Munz R.J. // J. Amer. Ceram. Soc. – 1997. – **80**. – P. 2425.
8. Bradshaw S.M., Spicer J.L. // J. Amer. Ceram. Soc. – 1999. – **82**. – P. 2293.
9. Li J., Xia Y., Zhao M. et al. // J. Phys.: Condens. Matter. – 2007. – **19**. – P. 346228.
10. Chang C., Patzer A.B., Sedlmayr E. et al. // Chem. Phys. – 2001. – **271**. – P. 283.
11. Ioan S.D., Francisco L.O., Ionel H. // J. Mol. Struct. (THEOCHEM). – 1996. – **370**. – P. 17.
12. Frisch M.J., Trucks G.W., Schlegel H.B., Scuseria G.E., Robb M.A., Cheeseman J.R., Montgomery J.A. Jr., Vreven T., Kudin K.N., Burant J.C., Millam J.M., Iyengar S.S., Tomasi J., Barone V., Mennucci B., Cosci M., Scalmani G., Rega N., Petersson G.A., Nakatsuji H., Hada M., Ehara M., Toyota K., Fukuda R., Hasegawa J., Ishida M., Nakajima T., Honda Y., Kitao O., Nakai H., Klene M., Li X., Knox J.E., Hratchian H.P., Cross J.B., Adamo C., Jaramillo J., Gomperts R., Stratmann R.E., Yazyev O., Austin A.J., Cammi R., Pomelli C., Ochterski J.W., Ayala P.Y., Morokuma K., Voth G.A., Salvador P., Dannenberg J.J., Zakrzewski V.G., Dapprich S., Daniels A.D., Strain M.C., Farkas O., Malick D.K., Rabuck A.D., Raghavachari K., Foresman J.B., Ortiz J.V., Cui Q., Baboul A.G., Clifford S., Cioslowski J., Stefanov B.B., Liu G., Liashenko A., Piskorz P., Komaromi I., Martin R.L., Fox D.J., Keith T., Al-Laham M.A., Peng C.Y., Nanayakkara A., Challacombe M., Gill P.M.W., Johnson B., Chen W., Wong M.W., Gonzalez C., Pople J.A. Gaussian 03, revision C. 02. Gaussian, Inc., Pittsburgh PA, 2003.
13. Reed A.E., Curtiss L.A., Weinhold F. // Chem. Rev. – 1988. – **88**. – P. 899.
14. Quong A.A., Pederson M.R., Broughton J.Q. // Phys. Rev. B. – 1994. – **50**. – P. 4787.
15. Jiao H., Schleyer P.v.R., Mo Y. et al. // J. Amer. Chem. Soc. – 1997. – **119**. – P. 7075.
16. Charkin O.P., Klimenko N.M., Moran D. et al. // J. Phys. Chem. A. – 2002. – **106**. – P. 11594.